Molecular mechanisms of tolerance adaptation for *Saccharomyces cerevisiae* NRRL Y-50049

ZongLin Lewis Liu

Bioenergy Research Unit, National Center for Agricultural Utilization Research, USDA-ARS, Peoria, IL 61604 USA | ZLewis.Liu@ars.usda.gov

Background

A tolerant strain of NRRL Y-50049 was successfully obtained through environmental evolution at a laboratory setting from *Saccharomyces cerevisiae* NRRL Y-12632, a diploid industrial type strain also cataloged as ATCC 18824, AWRI74, CCRC 21447, DBVPG 6173, DSM 70449, IFO 10217, IGC 4455, JCM 7255, and NCYC 505 by world-wide collection centers. Strain Y-50049 is able to *in situ* detoxify 2-furaldehyde (furfural) and 5-hydroxymethyl-2-furaldehyde (HMF), major toxic chemicals derived from lignocellulose-to-fuels conversion, while producing ethanol. The adapted tolerance of Y-50049 is stable and has demonstrated as inheritable characteristics over more than a decade. Understanding molecular mechanisms underlying the adapted tolerance of Y-50049 will aid development of next-generation biocatalysts for low-cost production of advanced biofuels and a sustainable bio-based economy.

Mode of action

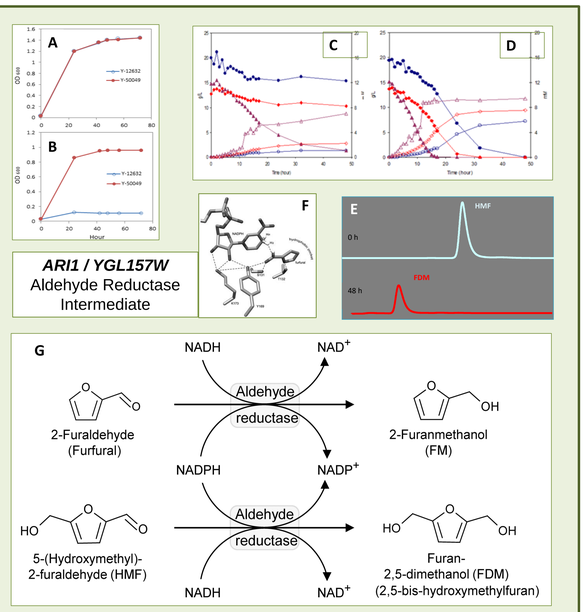

Fig. 1. Mode of action. A , B. Cell growth response of NRRL Y-50049 compared with its progenitor type strain *Saccharomyces cerevisiae* NRRL Y-12632 on an YM medium without (A) or with treatment (B) of furfural and HMF ; **C, D.** Dynamic metabolic conversion profiles of glucose (●), ethanol (O), HMF (◆), FDM (◇), furfural (▲), and FM (△) in the presence of HMF (C) and furfural (D) for Y-12632 (red and gray) vs Y-50049 (blue and purple); **E.** A reverse-phase HPLC chromatogram showing HMF detected by UV absorbance at 282 nm at 0 h and its conversion product of 2,5-bishydroxymethylfuran (furandimethanol, FDM) at 222 nm. No HMF recovered at 282 nm 48 h after the incubation with yeast; **F.** A novel aldehyde reductase gene *ARI1* was identified as the key gene for the aldehyde reduction and a model of Ari1p showing NADPH orientations; **G.** Conversion pathways of furfural and HMF into FM and FDM catalyzed by representative reductases coupled with NADPH and/or NADH [Liu et al. 2004; 2005; 2008; 2019; Liu and Moon 2009; Bowman et al. 2010; Jordan et al. 2011].

Key regulatory elements

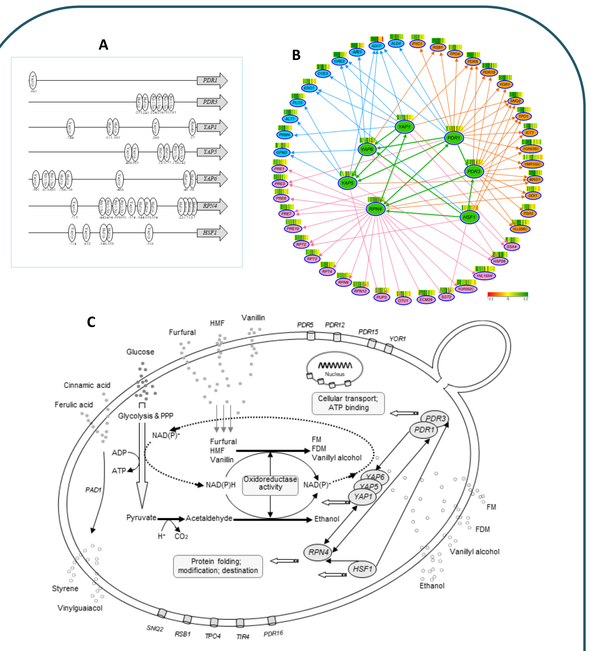

Fig. 2. Key regulatory elements. A. DNA binding sites for seven selective transcription factor genes *YAP1*, *YAP5*, *YAP6*, *PDR1*, *PDR3*, *RPN4*, and *HSF1* in the promoter regions (from -1000 to -1) showing overlapping motifs; **B.** Significant regulatory interactive networks among seven transcription factor genes (filled green and green arrows) and induced genes encoding functional reduction enzymes (filled blue and blue arrows), PDR gene family (filled orange and orange arrows), and proteasome function (filled pink and pink arrows). **C.** A prototype model showing global interactive relationships for key regulatory elements involved in three major functional gene categories for the tolerant Y-50049 resistant to furfural and HMF [Ma and Liu 2010; Liu 2011, 2018].

Cell wall integrity signaling pathway

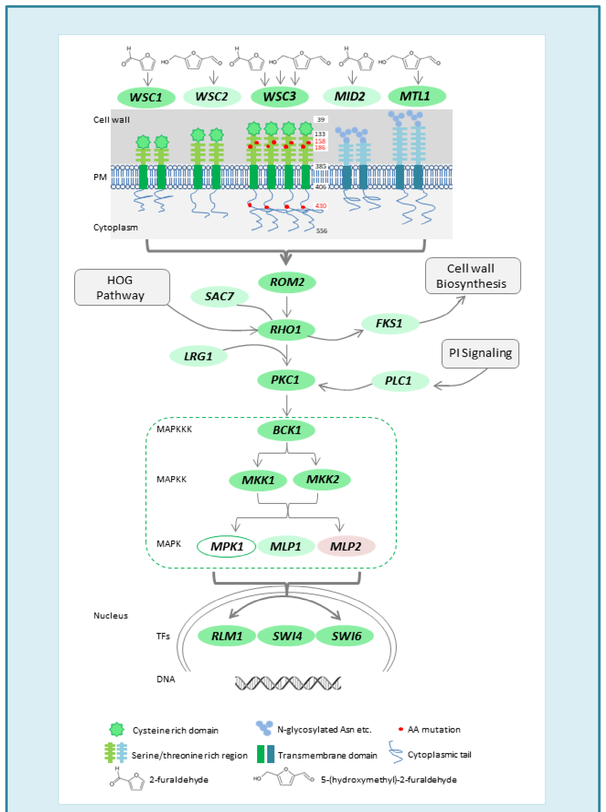

Fig. 3. Cell wall integrity signaling pathway. An illustration of a more robust cell wall integrity signaling pathway of the adapted Y-50049 in response to a synergistic challenge of furfural and HMF compared with a haploid laboratory model strain BY4741. Function domains of the sensor proteins are depicted including the cysteine rich domain, serine/threonine rich region, N-glycosylated asparagines and the respective residues, transmembrane domain, and cytoplasmic tail. Locations of the functional domains of Wsc3p are labeled relative to the cell wall and membrane. Relative locations of its deduced amino acid mutations are also labeled [Liu et al. 2018].

In situ detoxification pathway

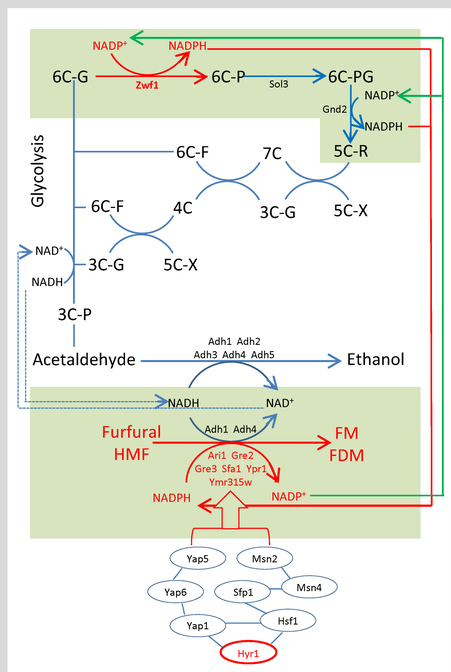

Fig. 4. *In situ* detoxification pathway. A fine-tuned *in situ* detoxification pathway of the adapted Y-50049 by comparative dynamic protein expression analysis showing a unique expression of Zwf1 in response to a synergistic challenge of furfural-HMF. The outstanding Zwf1 expression appeared to drive the sugar metabolism in favor of the irreversible oxidative branch of pentose phosphate pathway (PPP). Y-50049 also gained enhanced expression of a group of aldehyde reductases that enabled reduction of furfural and HMF into FM and FDM, respectively. Such a biotransformation by these enzymes consumed NADPH and released NADP+. The adapted Zwf1 reaction provided the essential cofactor NADPH for reduction of furfural and HMF (red line). In return, the biotransformation pathway released NADP+ supplying a smooth feedback to the oxidative branch of PPP (green line) that restored the cofactor imbalance caused by the toxic chemicals. The distinctly activated Hyr1, a redox signaling agent activating key transcription factor Yap1, is also presented in red in relationships with representative transcription factors at the bottom. 3C-G stands for glyceraldehydes 3-phosphate; 3C-P, pyruvate; 4C, erythrose 4-phosphate; 5C-R, ribose 5-phosphate; 5C-X, xylulose 5-phosphate; 6C-F, fructose 6-phosphate; 6C-G, glucose 6-phosphate; and 7C, sedoheptulose 7-phosphate [Liu et al. 2019].

Rewired transcription subnetworks

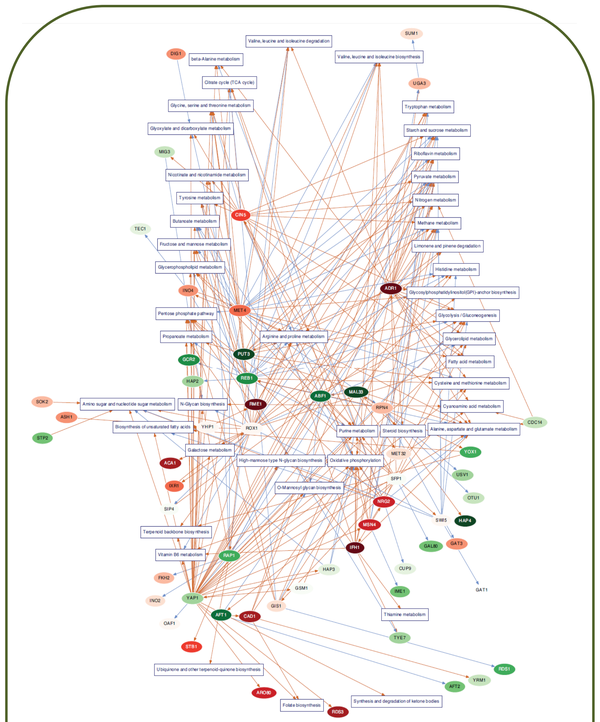

Fig. 5. Rewired transcription subnetworks. Rewired transcription networks showing significant impact of at least 44 downstream metabolic pathways for the adapted Y-50049 under challenges of furfural-HMF compared with its progenitor Y-12632. Oval nodes represent over- (green) or under- (red) expressed transcription factors in Y-50049. Brown edges indicate rewired and blue, conserved interactions across strain Y-50049 and its wild type parental strain NRRL Y-12632. An edge from a transcription factor to a metabolic pathway box denotes a significant interaction from the transcription factor to an enzyme-encoding gene on the pathway. Brown/Blue edges are statistically significantly rewired/conserved interactions across the two strains. All subnetworks before joining have adjusted heterogeneity *P*-value *P*D ≤ 0.05 [Zhang et al. 2015].

Table 1. Pathways in Y-50049 regulated by rewired upstream transcription subnetworks in response to the challenge of toxic chemicals

KEGG ID	Downstream metabolic pathway	Upstream subnetwork		Working zone Change
		Heterogeneity	Homogeneity	
	PD PC PZ			
sce00010	Glycolysis / Gluconeogenesis	0.00e+00	1.31e-14	1.08e-03
sce00290	Valine, leucine and isoleucine biosynthesis	0.00e+00	1.77e-10	2.49e-04
sce00520	Amino sugar and nucleotide sugar metabolism	0.00e+00	1.38e-11	2.52e-04
sce00620	Pyruvate metabolism	0.00e+00	1.31e-14	2.91e-04
sce00680	Methane metabolism	0.00e+00	3.46e-11	7.37e-04
sce00250	Alanine, aspartate and glutamate metabolism	6.55e-15	4.60e-11	2.17e-03
sce00030	Pentose phosphate pathway	1.97e-14	3.15e-09	1.30e-02
sce00190	Oxidative phosphorylation	4.59e-14	2.04e-12	7.98e-05
sce00330	Arginine and proline metabolism	4.59e-14	2.51e-11	7.93e-03
sce00280	Valine, leucine and isoleucine degradation	1.05e-13	1.68e-08	8.12e-04
sce00750	Vitamin B6 metabolism	1.11e-13	1.68e-09	5.96e-04
sce00260	Glycine, serine and threonine metabolism	2.69e-13	9.52e-11	1.04e-03
sce00410	beta-Alanine metabolism	2.82e-13	5.12e-07	1.74e-03
sce00910	Nitrogen metabolism	3.14e-13	9.04e-10	1.18e-03
sce00340	Histidine metabolism	3.60e-13	2.28e-10	7.51e-04
sce00650	Butanoate metabolism	4.98e-13	2.89e-13	3.09e-02
sce00640	Propanoate metabolism	6.03e-13	3.59e-08	1.64e-04
sce00500	Starch and sucrose metabolism	7.47e-13	1.11e-13	5.72e-03
sce00020	Citrate cycle (TCA cycle)	9.37e-13	4.04e-09	3.90e-03
sce00460	Cyanoamino acid metabolism	9.43e-13	1.94e-07	8.81e-04
sce00561	Glycerolipid metabolism	2.36e-12	2.37e-07	3.05e-04
sce00071	Fatty acid metabolism	2.66e-12	7.41e-06	4.35e-04
sce00051	Fructose and mannose metabolism	3.04e-12	2.77e-10	3.50e-02
sce00230	Purine metabolism	4.93e-12	3.50e-10	1.72e-02
sce00564	Glycerophospholipid metabolism	5.14e-12	2.18e-07	3.19e-03
sce00380	Tryptophan metabolism	8.36e-12	1.18e-05	1.52e-03
sce00900	Terpenoid backbone biosynthesis	8.57e-12	4.77e-05	2.85e-03
sce00760	Nicotinate and nicotinamide metabolism	1.11e-11	3.94e-05	1.96e-03
sce00740	Riboflavin metabolism	1.23e-11	1.01e-05	3.15e-03
sce00514	O-Mannosyl glycan biosynthesis	1.61e-11	1.65e-05	2.03e-03
sce01040	Biosynthesis of unsaturated fatty acids	3.87e-11	1.23e-04	1.81e-03
sce00052	Galactose metabolism	4.87e-11	3.31e-04	3.48e-04
sce00630	Glyoxylate and dicarboxylate metabolism	5.71e-11	5.15e-05	2.12e-03
sce00350	Tyrosine metabolism	1.89e-10	1.30e-07	1.11e-02
sce00270	Cysteine and methionine metabolism	1.91e-10	6.22e-09	1.65e-03
sce00563	Glycosylphosphatidylinositol(GPI)-anchor biosynthesis	2.51e-10	2.99e-05	1.55e-02
sce00730	Thiamine metabolism	3.35e-10	4.91e-05	7.02e-03
sce00513	High-mannose type N-glycan biosynthesis	6.37e-10	1.91e-03	3.68e-03
sce00510	N-Glycan biosynthesis	9.67e-10	1.38e-08	1.47e-02
sce00100	Steroid biosynthesis	2.01e-09	2.14e-01	2.95e-04
sce00903	Limonene and pinene degradation	5.63e-08	1.19e-03	5.05e-03
sce00790	Folate biosynthesis	5.85e-08	1.99e-01	3.64e-02
sce00130	Ubiquinone and other terpenoid-quinone biosynthesis	3.46e-07	7.22e-04	3.19e-03
sce00072	Synthesis and degradation of ketone bodies	7.93e-07	9.37e-03	8.27e-04

Pathway-based tolerance phenotypes

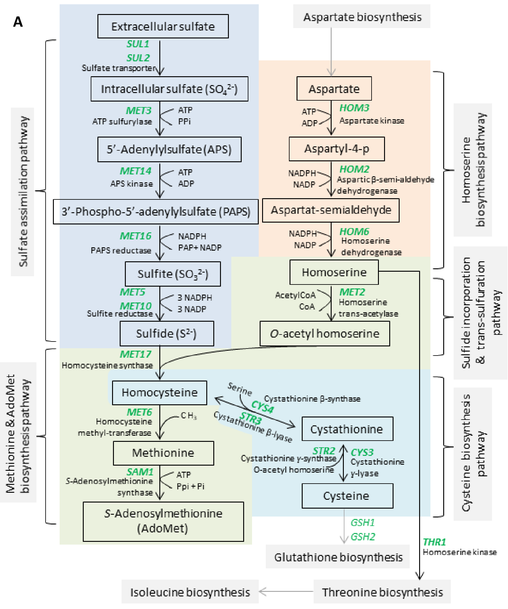

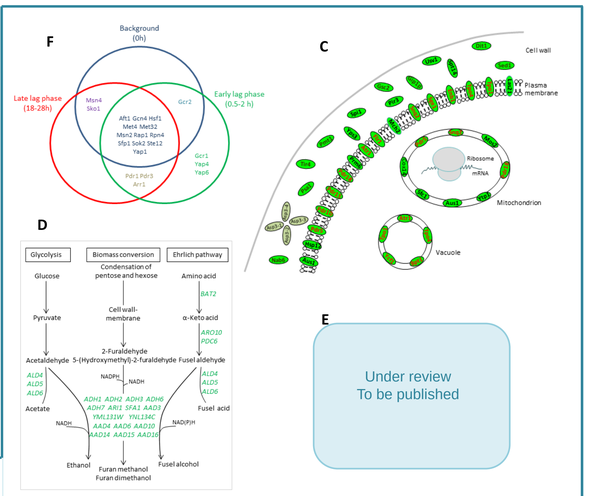

Fig. 6. Pathway-based tolerance phenotypes. A. Sulfur amino acid biosynthesis superpathway for the adapted Y-50049 showing increased transcription activity of important genes involved in sulfate assimilation and various closely related sulfur amino acid biosynthesis pathways; **B.** Enhanced REDOX with enzymatic and non-enzymatic defense systems of oxidative stress response for Y-50049 under stress of furfural-HMF. F-H ROS stands for furfural-HMF caused reactive oxygen species. Enzymatic defense system is boxed in gray and the non-enzymatic defense system in blank. Genes showing significantly enhanced expressions are bolded and key genes underlined; **C.** A prototype proposal of adaptive functions for genes involved in cell wall and membrane for Y-50049. Adapted candidate tolerant genes are marked in dark green. Transporter genes are presented in red and cell wall and membrane related genes in black; **D.** Induced gene expressions involved in endogenous and exogenous detoxification related to glycolysis-PPP and Erhlich pathway; **E.** ; **F.** Transcription factor genes with ETB (enhanced transcription background) from Y-50049 showing increased overlapping gene expressions that dominated the entire lag phase in response to the synergistic challenge of furfural-HMF. Background indicates transcription expression at 0 h prior to the furfural-HMF treatment. Early lag phase is defined as 0.5-2 h and late lag phase as 18-28 h after the furfural-HMF treatment [Liu and Ma 2020].

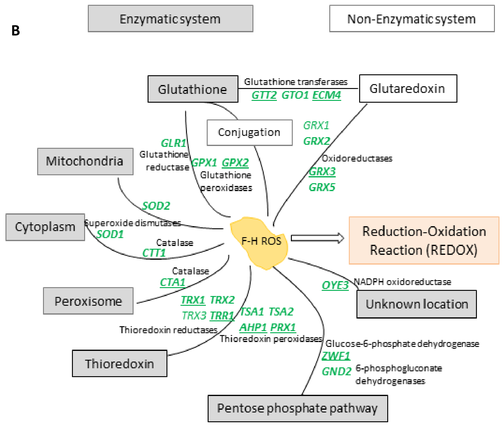

Conclusion and discussion

- ✓ The industrial yeast is more tolerant than lab model strains and the adapted Y-50049 demonstrated a more robust cell wall integrity signaling pathway.
- ✓ The industrial yeast has a plastic genome and can be adapted for long term applications that fit into specific ecological environment.
- ✓ The novel *ARI1* is a key gene and the renovated *in situ* detoxification pathway was the center mechanism of the adapted tolerance for Y-50049.
- ✓ Activated sulfur amino acid biosynthesis superpathway and enhanced enzymatic and non-enzymatic REDOX systems were accountable for the acquired tolerance of Y-50049.
- ✓ The yeast adaptation occurred at the genomic level with rewired networks and countless cross interactions.
- ✓ More reliable pathway-based tolerance phenotypes were suggested to replace single gene identifications on tolerance investigations.
- ✓ To be published

Methods

An integrated methodology of systematic biology approach was applied in more than a decade including conventional methods and advanced technologies at cellular, molecular and genomic levels, including bioinformatics, transcriptomics, phospholipidomics, and proteomics [see related references for details].

References

Liu ZL, Ma M (2020) Pathway-based signature transcriptional profiles as tolerant phenotypes for the adapted industrial yeast *Saccharomyces cerevisiae* resistant to furfural and HMF. Appl Microbiol Biotechnol https://doi.org/10.1007/s00253-020-10434-0

Liu ZL, Huang, X, Zhou Q, Xu J (2019) Protein expression analysis revealed a fine-tuned mechanism of *in situ* detoxification pathway for the tolerant industrial yeast *Saccharomyces cerevisiae*. Appl Microbiol Biotechnol 103:5781-5796

Liu ZL (2018) Understanding the tolerance of the industrial yeast *Saccharomyces cerevisiae* against a major class of toxic aldehyde compounds. Appl Microbiol Biotechnol 102:5369-5390

Liu, ZL, Wang X, Weber SA (2018) Tolerant industrial yeast *Saccharomyces cerevisiae* possess a more robust cell wall integrity signaling pathway against 2-furaldehyde and 5-(hydroxymethyl)-2-firaldehyde. J Biotechnol 276-277:15-24

Zhang Y, Liu ZL, Song M (2015) ChiNet uncovers rewired transcription subnetworks in tolerant yeast for advanced biofuels conversion. Nucleic Acids Res 43:4393-4407

Liu ZL (2012) Unification of gene expression data for comparable analysis under stress conditions. In: Liu ZL (ed) Microbial stress tolerance for biofuels: systems biology, Springer, Verlag Berlin Heidelberg, pp 279-299

Liu ZL, Moon J (2009) A novel NADPH-dependent aldehyde reductase gene from *Saccharomyces cerevisiae* NRRL Y-12632 involved in the detoxification of aldehyde inhibitors derived from lignocellulosic biomass conversion. Gene 446:1-10

Liu ZL, Ma M, Song M (2009) Evolutionarily engineered ethanologenic yeast detoxifies lignocellulosic biomass conversion inhibitors by reprogrammed pathways. Mol Genet Genomics 282:233-244